JACS
JOURNAL OF THE AMERICAN CHEMICAL SOCIETY

ARTICLE

pubs.acs.org/JACS

Dinuclear Silylium-enolate Bifunctional Active Species: Remarkable Activity and Stereoselectivity toward Polymerization of Methacrylate and Renewable Methylene Butyrolactone Monomers

Yuetao Zhang, Laura O. Gustafson, and Eugene Y.-X. Chen*

Department of Chemistry, Colorado State University, Fort Collins, Colorado 80523-1872, United States

ABSTRACT: Novel dinuclear silylium-enolate active species, consisting of an electrophilic silylium catalyst site and a nucleophilic silicon enolate initiating site that are covalently linked as single molecules, and their unique polymerization characteristics and kinetics are reported. Such unimolecular, bifunctional propagating species are conveniently generated from activation of ethyl- and oxo-bridged disilicon enolate (i.e., disilyl ketene acetal, di-SKA) compounds with $[Ph_3C][B(C_6F_5)_4]$. Both the ethyl- and oxo-bridged dinuclear species are much more active for the polymerization of methyl methacrylate (MMA) than the mononuclear SKA-based active species, exhibiting an approximate rate enhancement by a factor of 12 and 44, respectively. The oxo-bridged silylium-enolate species is considerably more active and controlled than the ethyl-bridged one, with their differences being even more pronounced in polymerizing a renewable monomer, γ-methyl-α-methylene-γ-butyrolactone. The polymerization by the oxo-bridged silylium-enolate active species follows first-order kinetics in both monomer and silylium catalyst concentrations, indicating a unimolecular propagation mechanism which involves an intramolecular delivery of the polymeric enolate nucleophile to the monomer activated by the silylium ion electrophile being placed in proximity in the same catalyst molecule. Highly stereoregular poly(methyl methacrylate) (PMMA), with a syndiotacticity up to 92% *rr*, can be produced in quantitative yield using the oxo-bridged propagator at low temperature.

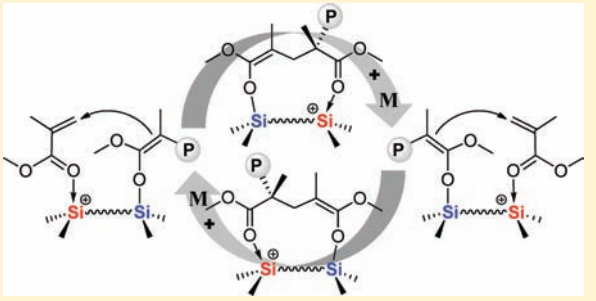

INTRODUCTION

Highly reactive silylium ions "R_3Si^+",[1] which are typically coordinated/stabilized by even very weak bases or donors, such as weakly coordinating anions, solvent molecules, monomers/substrates, or moieties in R, have shown diverse utilities in organic synthesis[2] and catalysis in general.[3] In terms of applications of silylium ions in polymerization catalysis, Olah and co-workers[4] have realized the cationic ring-opening polymerization (ROP) of cyclosiloxanes by trisilyloxonium ions that are generated by reacting R_3SiH with $[Ph_3C][B(C_6F_5)_4]$ {trityl tetrakis(pentafluorophenyl)borate, TTPB} in the presence of siloxanes; subsequent studies by other groups continued to address[5,6] the proposed propagation involving mainly the silyloxonium ions. Olah et al.[7] have also achieved the ROP of four-, six-, and seven-membered lactones using silylium-generating reagents such as {Me_3SiCl + $Na[B(3,5\text{-}(CF_3)_2C_6H_3)_4]$} and/or [$Me_3SiH$ + TTPB]. Recently, Manners, Reed, and co-workers[8] have reported the ROP of cyclic chlorophosphazene trimer $[N_3P_3Cl_6]$ catalyzed by silylium ions, paired with weakly coordinating halogenated carborane anions, with a typical 10 mol % catalyst loading.

Silylium ions are also known to catalyze polymerizations other than a ROP process. In this context, we[9] have demonstrated that R_3Si^+, generated either externally by the reaction of R_3SiH with TTPB or, *more significantly*, by in situ reaction of a silicon enolate (i.e., silyl ketene acetal, ^{R}SKA, $Me_2C{=}C(OMe)OSiR_3$) with a catalytic amount of TTPB, catalyzes living anionic-addition polymerization of polar conjugated olefins such as methyl methacrylate (MMA) at 25 °C, leading to poly(methyl methacrylate) (PMMA) with medium to high molecular weights ($M_n > 10^5$ g/mol) and narrow molecular weight distributions (MWD, defined by polydispersity index, PDI = M_w/M_n = 1.04−1.12).[9] Subsequent studies of structure−reactivity relationships for the polymerization of (meth)acrylates by [^{R}SKA + TTPB] have revealed a remarkable selectivity of ^{R}SKA (R = Me, Et, ^{i}Bu, Ph, Me_3Si) for monomer structure.[10] Specifically, the small Me_3Si^+ catalyst derived from ^{Me}SKA is highly active and efficient for the polymerization of MMA with a low catalyst loading of 0.05 mol %, giving a high catalyst turnover frequency (TOF) up to 1.5×10^3 h^{-1}, but it shows poor activity and efficiency for the polymerization of sterically less demanding, active α-proton-containing acrylates such as *n*-butyl acrylate (^{n}BA). In contrast, the larger $^iBu_3Si^+$ catalyst derived from ^{iBu}SKA exhibits low activity for the polymerization of MMA but exceptional activity, efficiency, and control for the polymerization of ^{n}BA, achieving quantitative ^{n}BA conversion in 1 min at 25 °C and giving an exceedingly high TOF up to 1.2×10^5 h^{-1}.[10] Such high polymerization activity and high to near quantitative catalyst efficiency achieved by these silylium catalysts are *noteworthy*

Received: June 9, 2011
Published: August 05, 2011

dx.doi.org/10.1021/ja2053573 | *J. Am. Chem. Soc.* 2011, 133, 13674–13684

Scheme 1. Initiation and Propagation Involved in Living/Controlled (Meth)acrylate Polymerization Catalyzed by R_3Si^+[9,10]

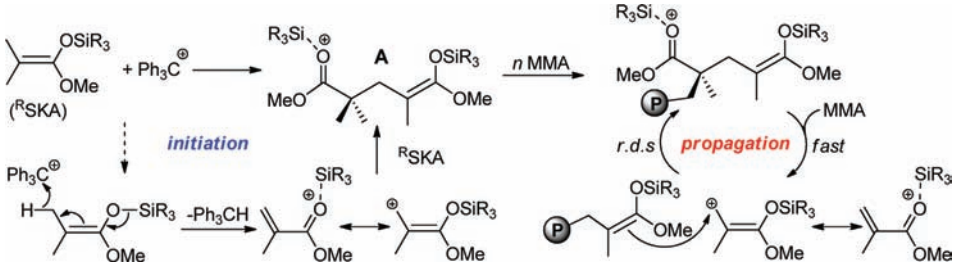

because they exceed those by cationic group 4 metallocenium and neutral lanthanocene catalysts, two catalyst classes widely regarded as most reactive and efficient for the coordination polymerization of (meth)acrylates.[11]

This silylium-catalyzed anionic-addition polymerization uses the precursory ^{R}SKA initiators which are commonly employed in the conventional group-transfer polymerization (GTP).[12] However, both chain initiation and propagation of the silylium-catalyzed polymerization are fundamentally different from those steps of GTP. Specifically, the initiation is uniquely "*monomerless*", which involves vinylogous hydride abstraction of ^{R}SKA by Ph_3C^+ leading to the R_3Si^+-activated MMA (i.e., activation of the initiator simultaneously generates the silylium catalyst and the activated monomer); subsequent Michael addition of ^{R}SKA to the silylated MMA generates the bifunctional active propagating species **A** (Scheme 1). The chain propagation consists of a fast step of recapturing the silylium catalyst from the ester group of the growing chain by the incoming MMA, followed by a rate-determining step (rds) of C−C bond coupling via intermolecular Michael addition of the polymeric SKA to the silylated MMA (Scheme 1). Furthermore, this silylium-catalyzed polymerization offers advantages over the conventional GTP in terms of its ability to readily produce high MW poly(methacrylate)s and effects living polymerization of acrylates under ambient temperature and low catalyst loading conditions.[9,10]

Several additional types of activators have also been used to deliver the silylium catalyst while activating ^{R}SKA. Recently, Kakuchi and co-workers[13] utilized a strong Brønsted acid, trifluoromethanesulfonimide ($HNTf_2$), to activate ^{R}SKA for in situ generation of Me_3SiNTf_2,[14] leading to the silylium-catalyzed living polymerization of MMA, and to activate dialkylaminosilyl enol ether for the living polymerization of *N*,*N*-dimethylacrylamide (DMAA).[15] The utility of $HNTf_2$ for generation of silylium ions has widely been realized in organic synthesis/catalysis by Yamamoto et al.[16] for catalytic Mukaiyama aldol and Michael reactions involving nucleophiles such as enol silyl ethers or SKA and acceptors such as aldehydes, ketones, or their α,β-unsaturated derivatives. The activity of the MMA polymerization by the [^{R}SKA + $HNTf_2$] system is rather low, most likely due to the coordinating nature of the Tf_2N^- anion, thus typically requiring 24 h reaction time and giving a low catalyst TOF of only ~80 h^{-1}.[13] We[17]employed strong Brønsted acids paired with super weakly coordinating perfluorophenylborate anions,[18] such as oxonium acid $[H(Et_2O)_2][B(C_6F_5)_4]$[19] and $[HN(Me_2)Ph][B(C_6F_5)_4]$,[20] as well as a strong Brønsted acid bearing a chiral disulfonimide counteranion,[2b] to deliver the R_3Si^+ catalyst. When paired with $[B(C_6F_5)_4]^-$, the silylium catalyst exhibits excellent activity with a high TOF of 6.0×10^3 h^{-1} for the MMA polymerization (or 6.4×10^4 h^{-1} for DMAA polymerization) using Me_3Si^+ or an exceptionally high TOF of 2.4×10^5 h^{-1} for the ^{n}BA polymerization using $^iBu_3Si^+$. Furthermore, the ^{R}SKA + $[H(Et_2O)_2][B(C_6F_5)_4]$ system achieves a high to quantitative catalyst efficiency and exhibits a high degree of control over M_n and MWD as well as an intriguing catalyst "self-repair" feature in the presence of moisture.[17] Interestingly, the more advanced GTP systems using the ^{R}SKA initiator and additionally employing different combinations of a Lewis acid and a Me_3Si-containing reagent, such as $[Me_3SiOTf + B(C_6F_5)_3]$,[21] $[Me_3SiI + HgI_2]$,[22] or $[Me_3SiI + RAl(OAr)_2]$,[23] are considerably more active than the typical GTP system using no such combinations, suggesting their possible involvement of the silylium-catalyzed process similar to what has been demonstrated for the ^{R}SKA + TTPB[9,10] and ^{R}SKA + $[H(Et_2O)_2][B(C_6F_5)_4]$ systems.[17] This revelation points to a possibly broad implication of the silylium-catalyzed polymerization process in the rapid and living/controlled polymerization of other polar conjugated olefins.

To extend the scope of monomers rapidly polymerizable by silylium catalysts, most recently we[24] investigated the polymerization of renewable methylene butyrolactones, such as α-methylene-γ-butyrolactone (MBL) and γ-methyl-α-methylene-γ-butyrolactone (MMBL). Considering an imminent challenge to gradually replace existing petroleum-based polymers with those derived from naturally renewable resources in a technologically and economically competitive fashion,[25] MBL and MMBL are of particular interest in exploring the prospects of substituting the petroleum-based methacrylate monomers for specialty chemicals and polymers production.[26] MBL, or tulipalin A, is a natural substance found in tulips, and the MBL ring is an integral building block of many (~10% known) natural products.[27] Its γ-methyl derivative MMBL can be readily prepared via a two-step process from the biomass-derived levulinic acid.[28] These two monomers have been successfully polymerized using various types of radical polymerization techniques,[29] group-transfer polymerization,[12b] anionic polymerization,[29l,30,31] polymerization by classical and frustrated Lewis pairs,[32] as well as coordination polymerization by metallocene[33] and half-metallocene[34] complexes. Using the silylium-catalyzed polymerization, our investigations into effects of ^{R}SKA (thus the resulting R_3Si^+ catalyst) and activator (thus the resulting counteranion) structures have revealed that the ^{iBu}SKA + TTPB combination is the most active and controlled system for (M)MBL polymerizations at ambient temperature, achieving a high TOF up to 1.2×10^4 h^{-1} and producing PMMBL with controlled low to high (M_n = 5.43 × 10^5 kg/mol) MW and narrow MWDs (PDI = 1.01−1.06).[24] Well-defined block copolymers of MBL and MMBL with MMA as well as block and statistical copolymers of MBL with MMBL have also been readily synthesized.

Scheme 2. Proposed Intramolecular vs Intermolecular Michael Addition Pathway for Dinuclear Silylium-enolate Active Species B

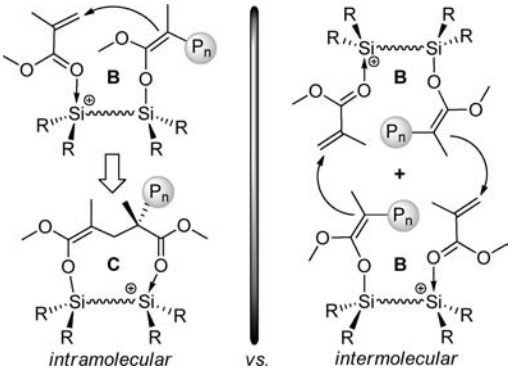

Significantly, the resulting atactic PMBL and PMMBL exhibit high glass transition temperatures (T_g's) of 194 and 225 °C, respectively, representing T_g enhancements of ~90 °C (for PMBL) and ~120 °C (for PMMBL) over the T_g of the typical atactic PMMA.[24]

Despite the above significant successes already achieved for the silylium-catalyzed polymerization of polar conjugated olefins, catalyst/initiator precursors ^{R}SKA employed so far are *mono*-SKA compounds (silicon enolates), which, upon activation, lead to propagating species **A** (Scheme 1) consisting of noncovalently bonded catalyst and initiating sites. As such, the bimolecular, activated monomer propagation mechanism (Scheme 1) imposes certain limitations on polymerizations under highly dilute initiator or catalyst conditions and on the stereochemical control of polymerization. We hypothesized that *covalently* linking electrophilic R_3Si^+ and nucleophilic SKA active sites into a single, dinuclear catalyst/initiator molecule such as **B** could overcome those limitations through converting the bimolecular-activated monomer propagation into a unimolecular process involving intermediate **C** formed by an *intramolecular* delivery of the SKA nucleophile to the monomer activated by the silylium ion electrophile being placed in proximity within the same molecule (Scheme 2). Alternatively, propagation could proceed via intermolecular Michael addition of **B** to another **B**. To ascertain these hypotheses and anticipate cooperativity or surprising effects often manifested by multinuclear catalysts in catalysis[35] for achieving superior activity and/or selectivity, the current work synthesized two types of di-SKA compounds having different linkages (Chart 1), examined their activation chemistry for the generation of the corresponding dinuclear silylium-enolate active species, and investigated their behavior and kinetics in the polymerization of polar conjugated olefins such as MMA and MMBL.

EXPERIMENTAL SECTION

Materials and Methods. All syntheses and manipulations of air- and moisture-sensitive materials were carried out in flamed Schlenk-type glassware on a dual-manifold Schlenk line, on a high-vacuum line, or in an argon- or nitrogen-filled glovebox. HPLC-grade organic solvents were sparged extensively with nitrogen during filling of the solvent reservoir and then dried by passage through activated alumina (for Et_2O, THF, and CH_2Cl_2) followed by passage through Q-5-supported copper catalyst (for toluene and hexanes) stainless steel columns. HPLC-grade DMF was degassed and dried over CaH_2 overnight, followed by vacuum transfer (not by distillation). NMR solvents $CDCl_3$ and DMSO-d_6 were dried over activated Davison 4-Å molecular sieves, and NMR spectra were recorded on a Varian Inova 300 MHz (FT 300 MHz, ^{1}H; 75 MHz, ^{13}C), a Varian Inova 400 MHz, or an Inova 500 MHz spectrometer. Chemical shifts for ^{1}H and ^{13}C spectra were referenced to internal solvent resonances and are reported as parts per million relative to $SiMe_4$, whereas ^{19}F NMR spectra were referenced to external $CFCl_3$. High-resolution mass spectrometry (HRMS) data were collected using an Agilent 6220 Accurate Time-of-flight LC/MS spectrometer.

Chart 1. Structures of Di-SKA Precatalysts and Polar Conjugated Olefins Employed in This Study

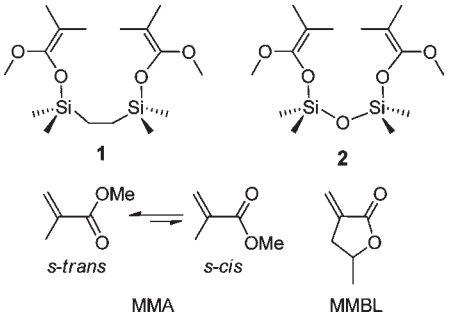

Monomers α-methylene-γ-butyrolactone (MBL) and γ-methyl-α-methylene-γ-butyrolactone (MMBL) were purchased from TCI America, while methyl methacrylate (MMA), dimethylketene methyl trimethylsilyl acetal (^{Me}SKA), diisopropylamine, and methyl isobutyrate were purchased from Sigma-Aldrich. These chemicals were degassed and dried over CaH_2 overnight, followed by vacuum distillation, while MMA was further purified by titration with neat tri(*n*-octyl)aluminum (Strem Chemical) to a yellow end point,[36] followed by vacuum distillation. Chlorotriisobutylsilane, 1,2-bis(chlorodimethylsilyl)ethane, 1,3-dichloro-1,1,3,3-tetramethyldisiloxane, and *n*-butyllithium were purchased from Sigma-Aldrich and used as received. Butylated hydroxytoluene (BHT-H, 2,6-di-*tert*-butyl-4-methylphenol) was purchased from Aldrich and was recrystallized from hexanes prior to use. Activator $[Ph_3C][B(C_6F_5)_4]$ (TTPB)[37] was obtained as a research gift from Boulder Scientific Co. and used as received. Modified literature procedures were employed to prepare activators $[H(Et_2O)_2][B(C_6F_5)_4]$[17,19] and trityl [tris(tetrachlorobenzenediolato)phosphate(V)], $[Ph_3C]$-[*rac*-TRISPHAT].[38]

Preparation of 1,2-Bis([(1-methoxy-2-methyl-1-propenyl)-oxy](dimethyl)silyl)ethane (1). Literature procedures for the synthesis of mono-SKAs[10] were modified for the preparation of di-SKA **1**. In a nitrogen-filled glovebox, a 200 mL Schlenk flask equipped with a stir bar was charged with THF (100 mL) and diisopropylamine (20.5 mL, 14.8 g, 146 mmol). This flask was sealed with a rubber septum, removed from the glovebox, interfaced to a Schlenk line, and placed in a 0 °C ice−water bath. ^{n}BuLi (96.0 mL, 1.6 M in hexane, 150 mmol) was added dropwise via syringe to the flask. Methyl isobutyrate (16.8 mL, 14.9 g, 146 mmol) was added to the above solution, after being stirred at 0 °C for 30 min. The resulting mixture was stirred at this temperature for 30 min, after which 1,2-bis(chlorodimethylsilyl)ethane (15.0 g, 70.0 mmol) was added. The mixture was allowed to warm slowly to room temperature and stirred overnight at this temperature, after which all volatiles were removed under vacuum. The resulting oil was dissolved in hexanes, and the resulting precipitates were filtered off under an argon atmosphere. The volatiles were once again removed, yielding the final product (21.0 g, 86.5%) as a yellow oil. ^{1}H NMR (C_6D_6, 400 MHz, 23 °C): δ 3.36 (s, 6H, O*Me*), 1.72 (s, 6H, =C*Me*$_2$), 1.68 (s, 6H, =C*Me*$_2$), 0.76 (s, 4H, SiC*H*$_2$), 0.22 (s, 12H, Si*Me*$_2$). ^{13}C NMR (C_6D_6, 100 MHz, 23 °C): δ 150.3 [=*C*(OMe)], 90.5 (=*C*Me$_2$), 56.4 (O*Me*),

17.0, 16.3 (=C*Me*), 8.1 ($SiCH_2$), −2.3 ($SiMe_2$). HRMS (APCI) *m*/*z* calcd for $C_{16}H_{34}O_4Si_2$ $[M + Na]^+$: 369.1888; found: 369.1891.

Preparation of 1,3-Bis([(1-methoxy-2-methyl-1-propenyl)-oxy])-1,1,3,3-tetramethyldisiloxane (2). The above same procedures were used for the preparation of di-SKA **2**, except for different reagents and amounts: diisopropylamine (10.3 mL, 7.40 g, 73.0 mmol), ^{n}BuLi (48.0 mL, 1.6 M in hexane, 75.0 mmol), methyl isobutyrate (8.4 mL, 7.50 g, 73.0 mmol), 1,3-dichloro-1,1,3,3-tetramethyldisiloxane (7.10 g, 35.0 mmol). The yield of the product, a yellow oil, was 8.8 g (75%). ^{1}H NMR ($CDCl_3$, 300 MHz, 23 °C): δ 3.52 (s, 6H, O*Me*), 1.57 (s, 6H, =C*Me*$_2$), 1.53 (s, 6H, =C*Me*$_2$), 0.21 (s, 12H, Si*Me*$_2$). ^{13}C NMR ($CDCl_3$, 75 MHz, 23 °C): δ 148.9 [=*C*(OMe)], 91.3 (=*C*Me$_2$), 56.9 (O*Me*), 17.0, 16.3 (=C*Me*), −0.5 (Si*Me*$_2$). HRMS (APCI) *m*/*z* calcd for $C_{14}H_{30}O_5Si_2$ $[M + Na]^+$: 357.1524; found: 357.1533.

Activation of Di-SKA 1 with TTPB. *In Situ Generation of Dinuclear Silylium-enolate Species [Ph_2C=C(CH=CH)$_2$CHCMe$_2$C-(OMe)=O···SiMe$_2$CH$_2$CH$_2$SiMe$_2$OC(OMe)=CMe$_2$][B(C_6F_5)$_4$] (**3**).* In an argon-filled glovebox, an NMR tube was charged with 5.8 mg (17 μmol) of di-SKA **1** and 0.3 mL of CD_2Cl_2. This NMR tube was sealed with a rubber septum, removed from the glovebox, and cooled to −78 °C. A 0.3 mL CD_2Cl_2 solution of TTPB (15.4 mg, 17 μmol) was slowly added to this tube via syringe. This reaction mixture was kept at −78 °C for 15 min. The reaction was monitored by taking NMR spectra being recorded from −80 °C to room temperature with 10 °C intervals after having equilibrated at each temperature for at least 15 min. Silylium-enolate **3** was formed cleanly at −80 °C; at temperatures ≥ −60 °C, some further reactions led to the formation of Ph_3CH (via vinylogous hydride abstraction by Ph_3C^+)[9] and several other unidentifiable species, with **3** still being the predominant species (>90% at −60 °C or >50% at RT) and complete consumption of it requiring more than 10 h at RT. The same reaction started directly at room temperature gave a spectrum rather similar to that of the controlled reaction starting at −78 °C and then gradually warming to room temperature. ^{1}H NMR (CD_2Cl_2, 300 MHz, −80 °C) for **3**: δ 7.31−7.21 (m, 6H, *m*,*p*-H, *Ph*), 7.09 (d, *J* = 7.5 Hz, 4H, *o*-H, *Ph*), 6.52 (d, *J* = 10.2 Hz, 2H, C(*CH*=CH)$_2$CH), 5.65 (dd, *J* = 10.2 and 3.0 Hz, 2H, C(CH=*CH*)$_2$CH), 4.32 (s, 3H, C(O*Me*)=O), 3.63 (s, 3H, C(O*Me*)=CMe$_2$), 3.46 (s, br, 1H, C(CH=CH)$_2$*CH*), 1.61 (s, 3H, C=C*Me*$_2$), 1.58 (s, 3H, C=C*Me*$_2$), 1.08 (s, br, 10H, C*Me*$_2$, CH_2CH_2), 0.47 (s, br, 12H, Si*Me*$_2$CH$_2$CH$_2$-Si*Me*$_2$). ^{19}F NMR (CD_2Cl_2, 282 MHz, −80 °C) for **3**: δ −133.9 (d, *J* = 12.1 Hz, 8F, *o*-F, C_6F_5), −162.9 (t, *J* = 19.7 Hz, 4F, *p*-F, C_6F_5), −166.9 (m, 8F, *m*-F, C_6F_5).

Activation of Di-SKA 2 with TTPB. *In Situ Generation of Dinuclear Silylium-enolate Species [Ph_2C=C(CH=CH)$_2$CHCMe$_2$C-(OMe)=O···SiMe$_2$OSiMe$_2$OC(OMe)=CMe$_2$][B(C_6F_5)$_4$] (**4**).* This reaction was carried out in the same manner as the reaction of di-SKA **1** with TTPB, showing the clean formation of silylium-enolate **4** at −80 °C. Likewise, at temperatures ≥−60 °C further reactions led to the formation of Ph_3CH and several other unidentifiable species. The reaction with 2 equiv of TTPB proceeded in the same fashion, cleanly producing silylium-enolate **4** at −80 °C, with another equiv of TTPB left unconsumed. ^{1}H NMR (CD_2Cl_2, 300 MHz, −80 °C) for **4**: δ 7.27−7.18 (m, 6H, *m*,*p*-H, *Ph*), 7.07 (d, *J* = 6.3 Hz, 4H, *o*-H, *Ph*), 6.51 (d, *J* = 10.2 Hz, 2H, C(*CH*=CH)$_2$CH), 5.63 (s, br, 2H, C(CH=*CH*)$_2$CH), 4.29 (s, 3H, C(O*Me*)=O), 3.62 (s, 3H, C(O*Me*)=CMe$_2$), 3.46 (s, br, 1H, C(CH=CH)$_2$*CH*), 1.37 (s, 6H, C=C*Me*$_2$), 1.07 (s, br, 6H, C*Me*$_2$), 0.60 (s, br, 6H, C(OMe)=O···Si*Me*$_2$OSiMe$_2$), 0.33 (s, br, 6H, C(OMe)=O···SiMe$_2$OSi*Me*$_2$). ^{19}F NMR (CD_2Cl_2, 282 MHz, −80 °C) for **3**: δ −133.9 (d, *J* = 12.4 Hz, 8F, *o*-F, C_6F_5), −162.8 (t, *J* = 21.4 Hz, 4F, *p*-F, C_6F_5), −166.8 (t, *J* = 18.3 Hz, 8F, *m*-F, C_6F_5).

Reaction of Di-SKA 2 with TTPB in the Presence of MMA. *Generation of Active Species **4** and PMMA.* In an argon-filled glovebox, an NMR tube was charged with 7.8 mg (23 μmol) of **2** and 0.3 mL of CD_2Cl_2. This NMR tube was sealed with a rubber septum, removed from the glovebox, and cooled to −78 °C. A 0.3 mL CD_2Cl_2 solution of TTPB (21.5 mg, 23 μmol) was slowly added to this tube via syringe. This reaction mixture was kept at −78 °C for 15 min. A 0.3 mL CD_2Cl_2 solution of MMA (2.3 mg, 23 μmmol) was slowly added to this tube. NMR spectra were recorded at −80 °C; at this temperature compound **4** and PMMA were formed cleanly. Another 20 equiv of MMA was added to this tube at −78 °C, and all MMA was completely consumed in 15 min to highly syndiotactic (∼91% *rr*) PMMA at this temperature.

General Polymerization Procedures. Polymerizations were performed in either 30 mL oven-dried glass reactors inside the glovebox for ambient temperature (∼25 °C) runs or 25 mL oven- and flame-dried Schlenk flasks interfaced to the dual-manifold Schlenk line for runs at other temperatures. In-reactor activation procedures[9,10,17] were employed for all polymerization runs. Specifically, a di-SKA and a monomer were premixed in toluene or CH_2Cl_2, and the polymerization was started by addition of a solution of activator TTPB, $[H(Et_2O)_2][B(C_6F_5)_4]$, or $[Ph_3C][$*rac*-TRISPHAT]. After the measured time interval, a 0.2 mL aliquot was withdrawn from the reaction mixture using a syringe and quickly quenched into a 1 mL vial containing 0.6 mL of undried "wet" $CDCl_3$ mixed with 250 ppm of BHT-H for obtaining the monomer conversion by ^{1}H NMR. The polymerization was immediately quenched by addition of 5 mL of 5% HCl-acidified methanol. The quenched mixture was precipitated into 100 mL of methanol, stirred for 1 h, filtered, washed with methanol, and dried in a vacuum oven at 50 °C overnight to a constant weight.

Specific Polymerization Example. In an argon-filled glovebox, a 30 mL, oven-dried glass reactor was charged with TTPB (10.8 mg, 11.7 μmol) in 5 mL of CH_2Cl_2. In a 20 mL glass vial di-SKA **2** (3.91 mg, 11.7 μmol) and MMA (1.00 mL, 9.35 mmol) were premixed in 4 mL of CH_2Cl_2. The mixture in the vial was rapidly poured into the reactor to start the polymerization at ambient temperature (∼25 °C). The [MMA]:[di-SKA]:[TTPB] ratio in this selected example was 800:1:1, giving rise to a [monomer (M)]/[initiator (I)] ratio of 800. The reaction was stirred at ambient temperature for 40 min, after which a 0.2 mL aliquot was withdrawn from the reaction mixture using syringe and quickly quenched into a 1 mL vial containing 0.6 mL of undried "wet" $CDCl_3$ mixed with 250 ppm of BHT-H. The reactor was taken out of the glovebox, and the reaction was quenched by addition of 5 mL of 5% HCl-acidified methanol. The quenched mixture was precipitated into 100 mL of methanol, stirred for 1 h, filtered, washed with methanol, and dried in a vacuum oven at 50 °C overnight to a constant weight. The quenched aliquot was analyzed by ^{1}H NMR to give 100% monomer conversion. The isolated and dried polymer was analyzed by gel permeation chromatography (GPC) to give M_n = 7.36 × 10^4 g/mol, PDI = 1.47, relative to the PMMA standards. The dried polymer was analyzed by ^{1}H NMR for its methyl triad distribution (tacticity). ^{1}H NMR ($CDCl_3$, 300 MHz, 23 °C) for PMMA: δ 3.60 (s, O*Me*), 1.98−1.82 (m, CH_2), 1.22 (s, Me, [*mm*] = 2.1%), 1.02 (s, Me, [*mr*] = 27.4%), 0.85 (s, Me, [*rr*] = 70.5%).

Polymerization Kinetics. Kinetic experiments were carried out in a stirred glass reactor at ambient temperature (∼25 °C) inside the glovebox using stock solutions of the reagents and the procedures described previously.[39]

Polymer Characterizations. Gel permeation chromatography (GPC) analyses of the polymers were carried out at 40 °C and a flow rate of 1.0 mL/min, with chloroform (for PMMA) or DMF (for PMMBL) as the eluent, on a Waters University 1500 GPC instrument coupled with a Waters RI detector and a Wyatt miniDAWN Treos LS detector equipped with four 5 μm PL gel columns (Polymer Laboratories). Chromatograms were processed with Waters Empower software (version 2002); number-average molecular weight (M_n) and polydispersity (M_w/M_n) of polymers were given relative to PMMA standards. Weight-average molecular weight (M_w) was obtained from the analysis of the LS data which were processed with Wyatt Astra

Scheme 3. Activation of di-SKA by TTPB for Generation of Dinuclear Silylium-enolate Active Species

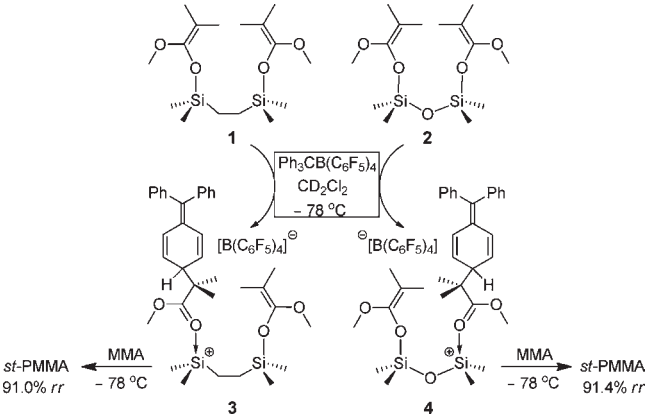

Software (version 5.3.2.15), and *dn*/*dc* values were determined assuming 100% mass recovery of polymers with known concentrations. ^{1}H NMR and ^{13}C NMR spectra for the analysis of PMMA microstructures were recorded in $CDCl_3$ at 50 °C and analyzed according to the literature methods,[40] while tacticities of PMBL[12b,24,29l] and PMMBL[24,30] were measured by ^{13}C NMR in DMSO-d_6 at 100 °C.

RESULTS AND DISCUSSION

Synthesis and Activation of Di-SKA. Ethyl-bridged di-SKA **1** (21 g) and oxo-bridged di-SKA **2** (8.8 g) were synthesized in a straightforward fashion by the reaction of the in situ generated lithium methyl isobutyrate with 1,2-bis(chlorodimethylsilyl)-ethane and 1,3-dichloro-1,1,3,3-tetramethyldisiloxane, respectively. The products were isolated through simple filtration, evaporation, and drying procedures (see Experimental Section), but they are not suitable for vacuum distillation as decomposition occurs at temperatures higher than 80 °C under vacuum.

Activation of the di-SKA precatalysts with activator TTPB in CD_2Cl_2 was carefully monitored by VT-NMR studies over a broad temperature window (from −78 to 25 °C). At −78 °C, the reaction of both **1** and **2** with TTPB leads to clean formation of dinuclear silylium-enolate active species **3** and **4** (Scheme 3), respectively. The reaction of di-SKA **2** with 2 equiv of TTPB at −78 °C did not produce a possible dication, with formation of dinuclear, monocation **4**, plus another equiv of TTPB left unreacted. Ethyl-bridged dinuclear silylium-enolate **3** is readily characterized by ^{1}H NMR, with characteristic resonances for the $[Ph_2C{=}C(CH{=}CH)_2CH{-}]$[9,41] moiety: δ 7.31−7.21 (m, 6H, *m*,*p*-H, *Ph*), 7.09 (d, 4H, *o*-H, *Ph*), 6.52 (d, 2H, C(C*H*=CH)$_2$CH), 5.65 (dd, 2H, C(*CH*=C*H*)$_2$CH), and 3.46 (s, br, 1H, C(CH=CH)$_2$C*H*); and for the $[{-}CMe_2C(OMe){=}O\cdots{}^{+}SiMe_2CH_2CH_2SiMe_2OC(OMe){=}CMe_2]$ moiety: δ 4.32 (s, 3H, C(O*Me*)=O), 3.63 (s, 3H, C(O*Me*)=CMe$_2$), 1.61 (s, 3H, C=C*Me*$_2$), 1.58 (s, 3H, C=C*Me*$_2$), 1.08 (s, br, 10H, C*Me*$_2$, C*H*$_2$C*H*$_2$), 0.47 (s, br, 12H, Si*Me*$_2$CH$_2$CH$_2$Si*Me*$_2$). The uncoordinated anion $[B(C_6F_5)_4]^-$ is readily recognizable from its characteristic resonances in ^{19}F NMR: δ −133.9 (d, 8F, *o*-F, C_6F_5), −162.9 (t, 4F, *p*-F, C_6F_5), −166.9 (m, 8F, *m*-F, C_6F_5). Oxo-bridged dinuclear silylium-enolate **4** is characterized in the same manner (see Experimental Section and Figure 1). Formation of **3** and **4** can be described as a result of electrophilic addition of Ph_3C^+, via the *para*-carbon of Ph, to the nucleophilic enolate carbon in the di-SKA.

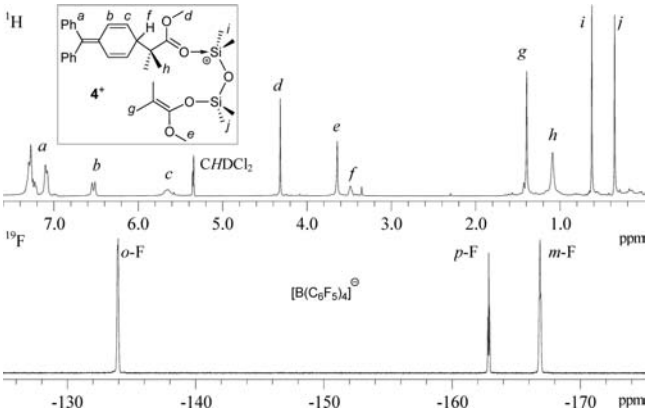

Figure 1. ^{1}H NMR (top) and ^{19}F NMR (bottom) spectra of dinuclear silylium-enolate **4** (CD_2Cl_2, −80 °C).

We previously observed the same reaction between a mono-SKA such as ^{Me}SKA with TTPB at −78 °C;[9] however, on warming to −70 °C the electrophilic addition product is being converted to propagating species **A** (Scheme 1), through vinylogous hydride abstraction by Ph_3C^+, followed by formal coupling of two SKA moieties, with concomitant formation of Ph_3CH, and is completely transformed to **A** at −50 °C. Behaving somewhat differently, electrophilic addition product **3** derived from di-SKA **1** begins to release Ph_3CH at temperatures ≥ −60 °C, accompanied by several other unidentifiable species plus predominantly the remaining **3**. Oxo-bridged dinuclear silylium-enolate **4** is more reactive with a much faster rate of decomposition (in the absence of monomer) at −60 °C or above. The high reactivity of dinuclear silylium-enolate active species **4** is nicely demonstrated by its ability to convert MMA quantitatively to highly syndiotactic (*st*-) PMMA (91.4% *rr*, vide infra) at −78 °C. Ethyl-bridged active species **3** can also polymerize MMA at −78 °C to highly syndiotactic PMMA (91.0% *rr*), but with lower activity (vide infra). In comparison, the active species **A** generated from mono-SKA exhibited no activity at temperatures below −20 °C. The reaction involving di-SKA **2**, TTPB, and MMA (in a stoichiometric amount or in excess) at −78 °C showed clean formation of **4** and PMMA and nothing else, *indicating the dinuclear silylium-enolate* **4** *is the active propagating species for this polymerization*.

MMA Polymerization Characteristics. Having determined the active species and their instability at ambient temperature in the absence of monomer, we began to investigate their performance in the polymerization of MMA at ambient temperature using the in-reactor activation procedures that ensure the active species, once generated, are in no time absent of monomer until completion of the reaction. Table 1 summarizes the selected results of the MMA polymerizations by the di-SKA system through in situ in-reactor activation with TTPB. It can be seen from the table that the polymerization by [di-SKA **1** + TTPB], with a TTPB (thus the silylium catalyst R_3Si^+) loading of 0.25 mol % with respect to monomer, is rapid, reaching 25.3% conversion in 20 s and giving a high initial TOF up to 1.8×10^4 h^{-1} (run 1); this TOF value corresponds to a 12-fold initial rate enhancement over the polymerization by the mono-SKA, ^{Me}SKA, which has a typical TOF of 1.5×10^3 h^{-1}.[9] On the other hand, unlike the living/controlled polymerization demonstrated

Table 1. Selected Results of MMA Polymerization by Di-SKA 1 and 2 Activated with TTPB [a]

run no.	di-SKA	[MMA]/[di-SKA]	TTPB (equiv)	time (min)	conv.[b] (%)	$10^{-3}M_n$[c] (g/mol)	PDI [c] (M_w/M_n)
1	**1**	400/1	1.0	0.33	25.3	11.3	1.71
2				0.67	35.3	14.6	1.59
4				1.0	43.7	16.2	1.44
5				1.5	48.1	18.3	1.37
6				2.0	57.1	20.5	1.40
7				3.0	65.3	22.7	1.39
8				4.0	69.6	23.7	1.39
9				7.0	76.8	25.5	1.40
10				10	80.5	27.9	1.38
11				20	86.4	28.4	1.40
12				40	90.9	28.9	1.40
13				60	91.1	27.5	1.46
14				300	97.4	27.5	1.43
15		400/1	0.1	31 (h)	42.1	18.8	1.28
16		800/1	1.0	23 (h)	79.8	49.9	1.42
17	**2**	400/1	1.0	0.33	92.4	n.d.	n.d.
18		400/1	1.0	1	100	47.4	1.29
19		800/1	1.0	5	100	73.6	1.47
20		1200/1	1.0	10	>99	99.0	1.55
21		1600/1	1.0	15	>98	116	1.65
22		2000/1	1.0	60	>96	140	1.69
23	**2**	1200/1.125	0.25	30	90.0	90.9	1.81
24		1200/0.875	0.25	60	97.2	106	1.84
25		1200/0.625	0.25	120	96.7	123	1.81
26		1200/0.375	0.25	240	90.6	209	1.74

[a] Carried out at ambient temperature (~25 °C) in 9 mL CH_2Cl_2 and 1 mL MMA solutions, where $[MMA]_0$ = 0.935 M. n.d. = not determined. [b] Monomer conversions measured by ^{1}H NMR. [c] M_n and PDI determined by GPC relative to PMMA standards.

for the mono-SKA system, the polymerization by di-SKA **1** was not controlled, producing PMMA with relatively broad MWDs ranging from PDI = 1.2 to 1.7. While there was an initial increase in MW with an increase in monomer conversion up to ~80% (runs 1 to 10), at higher conversions the polymer MW did not change any further appreciably. This observation, coupled with the measured M_n being considerably lower (by ~1.5 times) than the calculated M_n based on the [monomer (M)]/[initiator (I)], indicates the presence of chain transfer, which is more pronounced at the higher monomer conversion regime. Note that, given the di-SKA activation mechanism described above, a polymerization with an $x[M]_0/y[\text{di-SKA}]_0/z[\text{TTPB}]_0$ ratio will have the total equivalency of the silylium catalyst = z and the initiating enolate = $2(y - z) + z = 2y - z$, thereby giving a [M]/[I] ratio of $x/(2y - z)$.

The polymerization using just 0.1 equiv of TTPB with respect to 1 equiv of di-SKA **1** and 400 MMA (i.e., 0.025 mol % silylium catalyst) was much slower (TOF = 54 h^{-1}, run 15) than the reactions using 1 equiv of TTPB, but the PMMA produced at 42% conversion had a MW that is similar to the MW of the PMMA produced by the polymerization by 1 equiv of TTPB at the similar conversion (run 15 vs 4), suggesting the polymer MW is not sensitive to the amount of catalyst employed. On the other hand, when the [MMA]/[**1**] ratio (which is the same as the [M]/[I] ratio as $y = z$ for these two runs) was increased by 2-fold from 400 to 800, the MW of the PMMA was nearly doubled at a similar monomer conversion of ~80% ($M_n = 2.79 \times 10^4$ g/mol for run 10 vs $M_n = 4.99 \times 10^4$ g/mol for run 16). All the polymers produced by this di-SKA system at ambient temperature are syndio-biased, having a methyl triad distribution of ~70% *rr*, ~28% *mr*, and ~2% *mm*, due to the chain-end control nature of this polymerization.

Several aspects of the polymerization show that oxo-bridged silylium-enolate **4** derived from di-SKA **2** is much more active and controlled than ethyl-bridged silylium-enolate **3** derived from di-SKA **1**. First, the polymerization by [**2** + TTPB] is about 3.7 times faster than [**1** + TTPB]. Thus, the MMA polymerization with the same catalyst loading of 0.25 mol % reached 92.4% conversion in 20 s (run 17), giving a very high initial TOF of 6.6×10^4 h^{-1}, which corresponds to a 44-fold rate enhancement over the polymerization by the mono-SKA system. Second, upon achieving quantitative conversion under 1 min, the polymer had $M_n = 4.74 \times 10^4$ g/mol (run 18), giving a good initiator efficiency, defined by $I^* = M_n(\text{calcd})/M_n(\text{exptl})$, where $M_n(\text{calcd}) = \text{MW(M)} \times [M]_0/[I]_0 \times \text{conversion \%} + \text{MW of chain end groups}$ (221), of 85%. Third, the experiments that examine the degree of control over polymer MW by varying the [M]/[I] ratio from 400 (0.25 mol % catalyst loading) to 2000 (0.05 mol % catalyst loading) showed that the polymerizations at all ratios achieved quantitative to near quantitative monomer conversions in short times, ranging from 1 min to 1 h, depending on the catalyst loading (runs 18–22) and that the polymer MW increased linearly (R^2 = 0.995) from $M_n = 4.74 \times 10^4$ g/mol to $M_n = 1.40 \times 10^5$ g/mol with increasing [M]/[I] ratio from 400 to 2000 (Figure 2). Fourth, a different set of experiments that employed a much lower, but constant, catalyst loading of

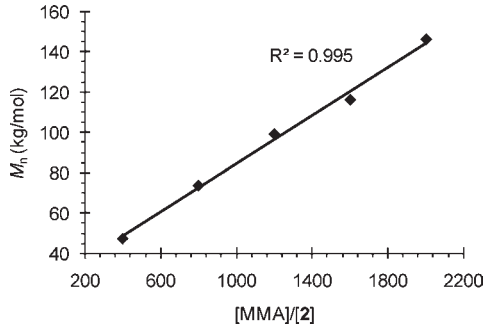

Figure 2. Plot of M_n of PMMA vs the [M]/[**2**] ratio (which is the same as the [M]/[I] ratio as $y = z$ for these runs) for the polymerization of MMA by the di-SKA **2** + TTPB (1:1) in CH_2Cl_2 at 25 °C (runs 18−22, Table 1).

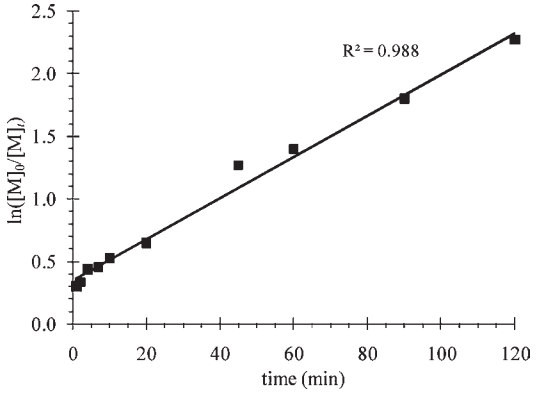

Figure 3. First-order kinetic plots of $\ln([M]_0/[M]_t)$ for the MMA polymerization by the di-SKA **2** + TTPB system in CH_2Cl_2 at −78 °C: $[MMA]_0$ = 0.935 M; $[\mathbf{2}]_0 = [TTPB]_0$ = 2.34 mM.

0.0208 mol % (0.25 equiv relative to 1200 equiv of MMA) and a varied amount of di-SKA **2** ranging from 1.125 to 0.375 equiv (runs 23−26), which corresponds to changing the [M]/[I] ratio from 600 to 2400, respectively, also showed that the polymer MW increased linearly (R^2 = 0.994) from medium $M_n = 9.09 \times 10^4$ g/mol to high $M_n = 2.09 \times 10^5$ g/mol.

Overall, the above results clearly show that the polymerization systems based on di-SKA **1** and **2** are much more active than the mono-SKA system, especially under high [M]/[I] ratio or low catalyst loading conditions. Also significant, the polymerization system based on oxo-bridged di-SKA **2** is not only considerably more active but also more controlled than the system based on ethyl-bridged di-SKA **1**. As both di-SKA systems follow the same initiation (vide supra) and propagation (vide infra) pathways, the observed large differences in the polymerization activity and control are presumably due to the resulting dialkyloxy silylium catalyst in **4** being more reactive—by virtue of inductive electron-withdrawing effects of the oxygen atom—than the trialkyl silylium catalyst in **3** and their relative proximity between the silylium catalyst and enolate initiating sites (i.e., two-carbon linkage in **3** vs one-oxygen linkage in **4**).

Polymerization Kinetics and Propagation Mechanism. We first profiled the MMA polymerization by the di-SKA **2** + TTPB system ([MMA]/[**2**]/[TTPB] = 400/1/1) in CH_2Cl_2 at −78 °C, the results of which clearly showed the first-order

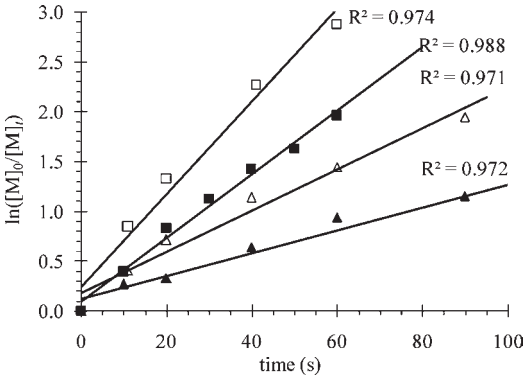

Figure 4. First-order kinetic plots of $\ln([M]_0/[M]_t)$ for the MMA polymerization by the di-SKA **2** + TTPB system in CH_2Cl_2 at 25 °C: $[MMA]_0$ = 0.935 M; $[\mathbf{2}]_0 = [TTPB]_0$ = 0.47 mM (▲), 0.58 mM (Δ), 0.78 mM (■), 1.17 mM (□).

dependence on monomer concentration (Figure 3). Subsequent detailed kinetic experiments at ambient temperature kept the [di-SKA]/[TTPB] ratio constant (1:1) and employed the [MMA]/[di-SKA] ratio ranging from 400 to 800 for di-SKA **1** or from 800 to 2000 for di-SKA **2**. The results showed the first-order dependence on monomer concentration [M], for all the ratios employed herein and for both di-SKA **1** and **2**. Figure 4 summarized the first-order kinetic plots for the polymerization by *x*MMA/**2** (x = 800, 1200, 1600, and 2000) at 25 °C and used the monomer conversion data from the early stage polymerization (≤90 s) to minimize effects of any potential side reactions at the late stage of the polymerization. There was no clear induction period observed for the polymerization at ambient temperature, and the first-order kinetics with respect to [M] held true for all the ratios investigated. This observation is in sharp contrast to the zero-order dependence on [M] observed for the polymerization systems based on the mono-SKA[9,10,24] and the μ-oxo-bridged dinuclear zirconocene,[42] pointing to a different propagation mechanism for the di-SKA polymerization system (vide infra).

In a different set of experiments, monomer concentration $[M]_0$ was fixed to be 0.935 M, while concentration of the activator, $[TTPB]_0$, thus the resulting silylium catalyst concentration, $[R_3Si^+]_0$, was varied from 0.19 to 1.17 mM. Initial initiator (silicon enolate moiety) concentration (0.78 mM) was kept constant for a fixed [M]/[I] ratio of 1200, by adjusting the di-SKA concentration $[\mathbf{2}]_0$ according to variations made in [TTPB] (i.e., $2 \times [\mathbf{2}]_0 - [TTPB]_0$) for each run. All runs that used the monomer conversion data from the early stage polymerization (≤60 s) again showed the first-order kinetic dependence on [M] as anticipated (Figure 5). A double logarithm plot of the apparent rate constants (k_{app}), obtained from the slopes of the best-fit lines to the plots of $\ln([M]_0/[M]_t)$ vs time as a function of [TTPB], was fit to a straight line (R^2 = 0.992) with a slope of 1.07 (inset, Figure 5). Thus, the kinetic order with respect to $[R_3Si^+]$, given by the slope of ∼1, reveals that the propagation is also first order in silylium catalyst concentration.

Overall, the observed first-order kinetics in both concentrations of monomer and catalyst, coupled with the structure of the active species **B** identified for this polymerization system, are consistent with an intramolecular Michael addition propagation mechanism depicted in Scheme 4. Specifically, this unimolecular

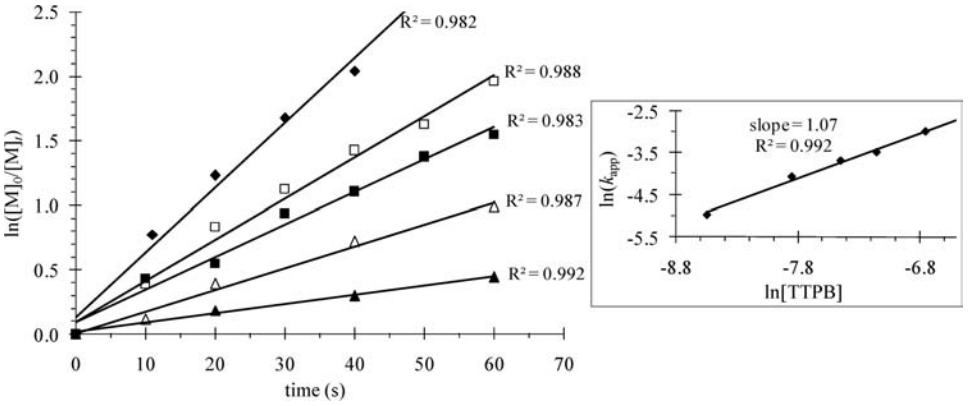

Figure 5. First-order kinetic plots of $\ln([M]_0/[M]_t)$ for the MMA polymerization by the di-SKA **2** + TTPB system in CH_2Cl_2 at 25 °C: $[MMA]_0$ = 0.935 M; $[TTPB]_0$ = 0.19 mM (▲), 0.38 mM (Δ), 0.58 mM (■), 0.78 mM (□), 1.17 mM (♦); $[\mathbf{2}]_0$ = 0.49 mM (▲), 0.58 mM (Δ), 0.68 mM (■), 0.78 mM (□), 0.97 mM (♦). Inset: plot of $\ln(k_{app})$ vs $\ln[TTPB]_0$.

Scheme 4. Proposed Propagation "Catalysis" Cycle for MMA Polymerization Catalyzed by Dinuclear Silylium-enolate Active Species

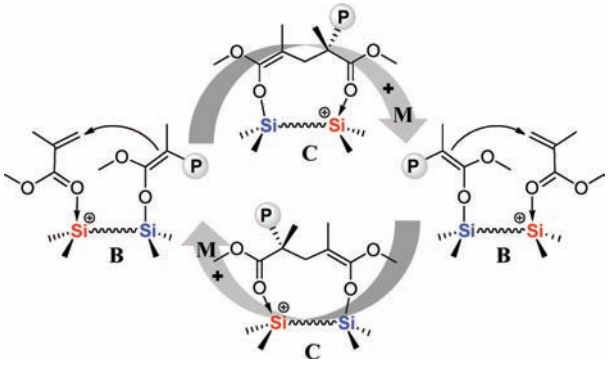

process involves propagating intermediate **C**, formed by an intramolecular delivery of the polymeric enolate nucleophile to the monomer activated by the silylium ion electrophile in the same silylium-enolate active species **B**. The first-order dependence on [M] also implies that the release of the silylium catalyst from its coordination to the penultimate ester group of the growing polymer chain (i.e., intermediate **C**) to the incoming monomer M is rate-limiting. This unimolecular propagation is reminiscent of the unimetallic mechanism established for the MMA polymerization by cationic group 4 *ansa*-metallocene catalysts.[11,39b,43] The alternative intermolecular Michael addition mechanism involving two **B** active centers (cf. Scheme 2) would give the second-order kinetics in catalyst concentration and the zero-order dependence on [M], assuming the same behavior as the analogous active species **A** (cf. Scheme 1). Furthermore, the latter bimolecular pathway, which involves two silylium cation centers in the transition state, should be energetically less favored; it is also inconsistent with the distinctively different, much superior polymerization performances observed for dinuclear active species **B**, relative to the mono-SKA system, which adopts the latter bimolecular propagation pathway.

MMBL Polymerization Characteristics. Having established the high activity of dinuclear silylium-enolate active species derived from di-SKA **1** and **2** for MMA polymerization, next we investigated characteristics of such active species for the polymerization of the renewable MMBL in CH_2Cl_2. The results on the polymerization of MBL were not included herein because the resulting polymer is insoluble in CH_2Cl_2, thus a heterogeneous process; polar, donor solvents such as DMF (in which PMBL is soluble) deactivate the silylium catalyst through strong adduct formation, thus shutting down the polymerization.[24] Table 2 summarizes the selected results of polymerizations of MMBL in CH_2Cl_2 by di-SKA **1** and **2** with TTPB activation.

With a catalyst loading of 0.25 mol % and a [M]/[I] ratio of 400, the MMBL polymerization by [di-SKA **1** + TTPB] at 25 °C achieved 43.4% conversion in 10 min, giving an initial TOF of 1.4×10^3 h^{-1} (run 27). However, the active species was largely deactivated at this point as there was no further significant improvement in conversion from this point forward, even after extended reaction times up to 24 h, at which time the conversion was only slightly higher (48.7%) and the PMMBL had M_n = 2.15×10^4 g/mol with PDI = 1.53 (run 28), which was close to the calculated M_n of 2.20×10^4 g/mol according the [M]/[I] ratio and the conversion data. Lowering the catalyst loading by 10-fold to 0.025 mol % (runs 29 and 30) or by 20-fold to 0.0125 mol % (runs 31 and 32) did not improve the polymerization significantly, achieving <60% conversion regardless of polymerization time. Considering the catalyst site in dinuclear silylium-enolate **3** being a Me_3Si^+-like silylium ion, these results are not surprising because we have previously shown that the small Me_3Si^+ catalyst is highly active and efficient for the polymerization of MMA but inefficient for the polymerization of the sterically less demanding monomers such as ^{n}BA or (M)MBL.[9,10,24]

Moving to oxo-bridged dinuclear active species **4** derived from activation of di-SKA **2** by TTPB, the polymerization with a catalyst loading of 0.25 mol % and a [M]/[I] ratio of 400 at 25 °C achieved 78% conversion in just 2 min, giving an initial TOF of 9.36×10^3 h^{-1} (run 33). This TOF value was about 6.7 times higher than that observed for **3**, but the same catalyst deactivation behavior was observed (run 34). Lowering the catalyst loading by half to 0.125 mol % achieved similar conversions but at shorter times; for example, 79.9% conversion was achieved in 1 min, giving a high TOF of 3.84×10^4 h^{-1} (run 35). On the other hand, decreasing the [M]/[I] ratio to 200, near quantitative conversions were achieved in 1 min (98.4%, run 37) and 30 min (98.0%, run 38) at 25 and 0 °C, respectively, or a quantitative

Table 2. Selected Results of MMBL Polymerization by Di-SKA 1 and 2 Activated with TTPB [a]

run no.	di-SKA	[M]/[di-SKA]/[TTPB]	temp (°C)	time (min)	conv.[b] (%)	$10^{-3}M_n$[c] (g/mol)	PDI[c] (M_w/M_n)
27	**1**	400/1/1	25	10	43.4	n.d.	n.d.
28	**1**	400/1/1	25	1440	48.7	21.5	1.53
29	**1**	400/1/0.1	25	10	51.0	n.d.	n.d.
30	**1**	400/1/0.1	25	1440	58.9	23.2	1.42
31	**1**	400/1/0.05	25	10	30.0	n.d.	n.d.
32	**1**	400/1/0.05	25	1380	49.5	21.4	1.41
33	**2**	400/1/1	25	2	78.0	n.d.	n.d.
34	**2**	400/1/1	25	1440	82.8	50.2	1.64
35	**2**	400/1/0.5	25	1	79.9	n.d.	n.d.
36	**2**	400/1/0.5	25	60	81.9	42.6	1.64
37	**2**	200/1/1	25	1	98.4	26.1	2.07
38	**2**	200/1/1	0	30	98.0	32.9	1.63
39	**2**	200/1/1	−78	360	100	36.6	1.36

[a] Carried out in 4.5 mL CH_2Cl_2 and 0.5 mL MMBL solutions. n.d. = not determined. [b] Monomer conversions (conv.) measured by ^{1}H NMR. [c] M_n and MWD determined by GPC relative to PMMA standards.

Table 3. Selected Results of MMA Polymerization by Di-SKA 2 with Different Activators at Varied T_P [a]

run no.	act	[M]/[**2**]/[act]	solvent	temp (°C)	time (min)	conv.[b] (%)	$10^{-3}M_n$[c] (g/mol)	PDI[c] (M_w/M_n)	[*rr*][b] (%)	[*mr*][b] (%)	[*mm*][b] (%)
40	**a**	1200/0.75/0.5	DCM	25	30	98.0	114	1.69	70.0	28.0	2.0
41	**b**	1200/0.75/0.5	DCM	25	60	80.3	165	1.79	70.7	27.0	2.3
42	**c**	1200/0.75/0.5	DCM	25	60	63.9	287	1.53	70.8	27.1	2.1
43	**a**	800/1/1	DCM	25	5	100	73.6	1.47	70.5	27.4	2.1
44	**a**	800/1/1	DCM	0	30	100	133	1.37	75.6	23.1	1.3
45	**a**	800/1/1	DCM	−78	1440	100	142	1.54	91.4	7.2	1.4
46	**b**	800/1/1	DCM	−78	1440	100	184	1.60	92.0	7.5	0.5
47	**a**	800/1/1	TOL	−78	600	91.8	152	1.46	83.1	16.2	0.7
48	**b**	800/1/1	TOL	−78	1440	77.3	154	1.63	81.0	18.4	0.6

[a] Carried out in 9 mL CH_2Cl_2 (DCM) or toluene (TOL) and 1 mL MMA solutions. Activators (act): **a** = $[Ph_3C]^+[B(C_6F_5)_4]^-$, **b** = $[Ph_3C]^+$-[Trisphat]$^-$, **c** = $[H(Et_2O)_2]^+[B(C_6F_5)_4]^-$. [b] Monomer conversions (conv.) and methyl triad distributions (*rr*, *mr*, *mm*) measured by ^{1}H NMR. [c] M_n and MWD determined by GPC relative to PMMA standards.

conversion in 6 h at −78 °C (run 39). For runs with [M]/[I] = 200, the PMMBL produced at 25 °C had $M_n = 2.61 \times 10^4$ g/mol, compared to the calculated M_n of 2.23×10^4 g/mol, while the polymers produced at lower temperatures had M_n's considerably higher than the calculated values.

Effects of Activator, Temperature, and Solvent. To explore the possibility of producing stereoregular polymers by the current novel unimolecular silylium-enolate catalyst initiator **4**, we examined effects of activator, temperature, and solvent on the tacticity of the resulting polymers. Table 3 summarizes the results of this study in the case of MMA polymerization.

Three types of activators examined in this study were TTPB (run 40), $[Ph_3C]$[*rac*-TRISPHAT] containing the racemic, hexacoordinate bulky chiral phosphate anion (run 41), and Brønsted acid activator $[H(Et_2O)_2][B(C_6F_5)_4]$ (run 42). Using an identical catalyst loading of 0.0417 mol % and a [M]/[I] ratio of 1200, the polymerizations at 25 °C in CH_2Cl_2 by all three activators gave PMMA with the same syndiotactic-biased tacticity of 70−71% *rr*, 27−28% *mr*, and ∼2% *mm* (runs 40−42). On the other hand, the polymerization activity and the polymer MW differed sharply, with TTPB being the most effective (98% conversion in 30 min), producing PMMA with controlled $M_n = 1.14 \times 10^5$ g/mol and nearly quantitative $I^* = 103\%$ and with $[H(Et_2O)_2][B(C_6F_5)_4]$ being the least effective (64% conversion in 60 min), producing PMMA with uncontrolled $M_n = 2.87 \times 10^5$ g/mol and a low I^* of only 27%.

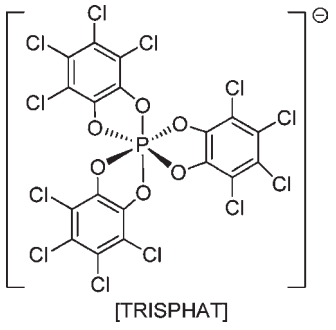

[TRISPHAT]

Next, we investigated temperature effects using the two better activators, TTPB and $[Ph_3C]$[*rac*-TRISPHAT], now with a catalyst loading of 0.125 mol % and a [M]/[I] ratio of 800 in CH_2Cl_2. At 25 °C using TTPB as activator, the resulting PMMA had *rr* = 70.5% (run 43) as anticipated; lowering the polymerization temperature to 0 °C noticeably increased the PMMA syndiotacticity to 75.6% *rr* (run 44). More significantly, a further decrease in the polymerization temperature to −78 °C yielded highly syndiotactic PMMA with *rr* = 91.4% (run 45), while still

achieving quantitative monomer conversion. In comparison, the polymerization by [di-SKA **1** + TTPB] at −78 °C was ∼4 times slower, although a similar polymer tacticity (91.0% *rr*) was also obtained. Likewise, the polymerization using activator $[Ph_3C]$-[*rac*-TRISPHAT] afforded highly syndiotactic PMMA with *rr* = 92.0% at −78 °C (run 46). Interestingly, replacing CH_2Cl_2 with toluene for polymerizations at −78 °C substantially lowered the syndiotacticity of PMMA by about 10% to *rr* = 83.1% (run 47) and 81.0% (run 45) for activators TTPB and $[Ph_3C]$[*rac*-TRISPHAT], respectively. This tacticity difference may be indicative of an ion-pairing strength effect on polymerization stereochemistry, considering the cation and anion are more tightly paired in the relatively nonpolar toluene than those in the more polar CH_2Cl_2.

CONCLUSIONS

This work has generated the novel dinuclear silylium-enolate active species derived from activation of di-SKA (silicon enolate) compounds with TTPB. These bifunctional active propagating species consist of the electrophilic silylium catalyst site and the nucleophilic silicon enolate initiating site that are covalently bonded as single molecules. Such unimolecular, dinuclear active species exhibit unique polymerization and kinetic characteristics as well as a rate enhancement by a factor of >40 and high stereoselectivity (at low temperature), as compared to the mononuclear SKA system. Key findings of this study are summarized as follows.

First, activation of ethyl- and oxo-bridged di-SKA **1** and **2** with 1 equiv of TTPB at −78 °C cleanly generates the corresponding dinuclear silylium-enolate **3** and **4** via electrophilic addition of Ph_3C^+ to the enolate carbon in the di-SKA. The reaction with 2 equiv of TTPB at −78 °C did not produce a possible dication. Addition of MMA to the preformed active species **4** at −78 °C forms highly syndiotactic (91.4% *rr*) PMMA in quantitative yield. In the absence of monomer, such active species are thermally unstable at temperatures ≥ −60 °C. In-reactor activation procedures employed in this study for all temperatures ensure the active species, once generated, are in no time absent of monomer until completion of the reaction.

Second, the MMA polymerization by ethyl-bridged dinuclear active species **3** [di-SKA **1** + TTPB] is about 12 times faster, but less controlled, than the mono-SKA system. Oxo-bridged dinuclear active species **4** [di-SKA **2** + TTPB] is about 3.7 times more active than **3**, reaching a high initial TOF of $6.6 \times 10^4\ h^{-1}$, which corresponds to a rate enhancement of 44-fold over the polymerization by the mono-SKA system. As the polymerization by **4** is also more controlled than that by catalyst **3**, polymers with low to high M_n ($>2 \times 10^5$ g/mol) can be readily produced by adjusting the [M]/[I] ratio. The observed large differences between these two dinuclear catalysts can be attributed to the resulting dialkyloxy silylium catalyst in **4** being more reactive, rendered by inductive electron-withdrawing effects of the oxygen atom, than the trialkyl silylium catalyst in **3** and to their relative proximity between the silylium catalyst and enolate initiating sites. The activity difference between these two dinuclear systems is even larger for the polymerization of the renewable methylene butyrolactone monomer, MMBL, with the TOF of **4** being about 6.7 times higher than that of **3**.

Third, the kinetic study of the polymerization in CH_2Cl_2 by active species **4** has shown that the polymerization follows first-order kinetics in both concentrations of monomer and catalyst. This kinetic result, coupled with the identification of the silylium-enolate active species, has yielded the unimolecular propagation mechanism, depicted in Scheme 4, which involves an intramolecular delivery of the polymeric enolate nucleophile to the monomer activated by the silylium ion electrophile being placed in proximity in the same catalyst molecule.

Fourth, among three types of activators examined for oxo-bridged di-SKA **2**, including TTPB, $[Ph_3C]$[*rac*-TRISPHAT], and $[H(Et_2O)_2][B(C_6F_5)_4]$, TTPB is the most effective with the highest activity and degree of control over the polymerization. On the other hand, the polymerizations in CH_2Cl_2 at 25 °C by all three activators produce PMMA with the same syndiotactic-biased tacticity of 70−71% *rr*. Significantly, while the active species **A** generated from mono-SKA exhibits no activity at temperature below −20 °C, the dinuclear active species are not only quite active in low temperatures but also produce highly stereoregular polymers. Hence, the MMA polymerization by di-SKA **2** in CH_2Cl_2 at −78 °C using activator TTPB and $[Ph_3C]$-[*rac*-TRISPHAT] affords highly syndiotactic PMMA, with syndiotacticity of *rr* = 91.4% and 92.0%, respectively. The unimolecular nature of the polymerization reaction rendered by the dinuclear silylium-enolate catalysts studied herein has provided a foundation for the future development of stereoselective polymerization using chiral silylium catalysts.

AUTHOR INFORMATION

Corresponding Author
eugene.chen@colostate.edu

ACKNOWLEDGMENT

This work was supported by the National Science Foundation (NSF-0848845). We thank Boulder Scientific Co. for the research gift of TTPB.

REFERENCES

(1) Selected reviews and recent examples: (a) Reed, C. A. *Acc. Chem. Res.* **2010**, *43*, 121–128. (b) Klare, H. F. T.; Bergander, K.; Oestreich, M. *Angew. Chem., Int. Ed.* **2009**, *48*, 9077–9079. (c) Duttwyler, S.; Do, Q.-Q.; Linden, A.; Baldridge, K. K.; Siegel, J. S. *Angew. Chem., Int. Ed.* **2008**, *47*, 1719–1722. (d) Küppers, T.; Bernhardt, E.; Eujen, R.; Willner, H.; Lehmann, C. W. *Angew. Chem., Int. Ed.* **2007**, *46*, 6346–6349. (e) Kochina, T. A.; Vrazhnov, D. V.; Sinotova, E. N.; Voronkov, M. G. *Russ. Chem. Rev.* **2006**, *75*, 95–110. (f) Müller, T. *Adv. Organomet. Chem.* **2005**, *53*, 155–215. (g) Kim, K.-C.; Reed, C. A.; Elliott, D. W.; Mueller, L. J.; Tham, F.; Lin, L.; Lambert, J. B. *Science* **2002**, *297*, 825–827. (h) Lambert, J. B.; Zhao, Y.; Zhang, S. M. *J. Phys. Org. Chem.* **2001**, *14*, 370–379. (i) Reed, C. A. *Acc. Chem. Res.* **1998**, *31*, 325–332. (j) Xie, Z.; Benesi, A.; Reed, C. A. *Organometallics* **1995**, *14*, 3933–3941. (k) Lambert, J. B.; Zhang, S.; Ciro, S. M. *Organometallics* **1994**, *13*, 2430–2443. (l) Xie, Z.; Liston, D. J.; Jelínek, T.; Mitro, V.; Bau, R.; Reed, C. A. *J. Chem. Soc., Chem. Commun.* **1993**, 384–386. (m) Lambert, J. B.; Zhang, S. *J. Chem. Soc., Chem. Commun.* **1993**, 383–384. (n) Lambert, J. B.; Zhang, S.; Stern, C. L.; Huffman, J. C. *Science* **1993**, *260*, 1917–1918.

(2) Selected recent examples: (a) Allemann, O.; Duttwyler, S.; Romanto, P.; Baldridge, K. K.; Siegel, J. S. *Science* **2011**, *332*, 574–577. (b) García-García, P.; Lay, F.; García-García, P.; Rabalakos, C.; List, B. *Angew. Chem., Int. Ed. Engl.* **2009**, *48*, 4363–4366. (c) Cheon, C. H.; Yamamoto, H. *J. Am. Chem. Soc.* **2008**, *130*, 9246–9247. (d) Hara, K.; Akiyama, R.; Sawamura, M. *Org. Lett.* **2005**, *7*, 5621–5623.

(3) Selected recent examples: (a) Müther, K.; Oestreich, M. *Chem. Commun.* **2011**, *47*, 334–336. (b) Klare, H. F. T.; Oestreich, M. *Dalton*

Trans. **2010**, *39*, 9176–9184. (c) Douvris, C.; Nagaraja, C. M.; Chen, C.-H.; Foxman, B. M.; Ozerov, O. V. *J. Am. Chem. Soc.* **2010**, *132*, 4946–4953. (d) Duttwyler, S.; Douvris, C.; Fackler, N. L. P.; Tham, F. S.; Reed, C. A.; Baldridge, K. K.; Siegel, J. S. *Angew. Chem., Int. Ed.* **2010**, *49*, 7519–7522. (e) Douvris, C.; Ozerov, O. V. *Science* **2008**, *321*, 1188–1190.

(4) (a) Wang, Q.; Zhang, H.; Prakash, G. K. S.; Hogen-Esch, T. E.; Olah, G. A. *Macromolecules* **1996**, *29*, 6691–6694. (b) Olah, G. A.; Li, X.-Y.; Wang, Q.; Rasul, G.; Prakash, G. K. S. *J. Am. Chem. Soc.* **1995**, *117*, 8962–8966.

(5) Toskas, G.; Moreau, M.; Masure, M.; Sigwalt, P. *Macromolecules* **2001**, *34*, 4730–4736.

(6) Cypryk, M.; Chojnowski, J.; Kurjata, J. *ACS Symp. Ser.* **2007**, *964*, 10–26.

(7) Olah, G. A.; Wang, Q.; Li, X.-Y.; Rasul, G.; Prakash, G. K. S. *Macromolecules* **1996**, *29*, 1857–1861.

(8) Zhang, Y.; Huynh, K.; Manners, I.; Reed, C. A. *Chem. Commun.* **2008**, 494–496.

(9) Zhang, Y.; Chen, E. Y.-X. *Macromolecules* **2008**, *41*, 36–42.

(10) Zhang, Y.; Chen, E. Y.-X. *Macromolecules* **2008**, *41*, 6353–6360.

(11) Chen, E. Y.-X. *Chem. Rev.* **2009**, *109*, 5157–5214.

(12) (a) Webster, O. W. *Adv. Polym. Sci.* **2004**, *167*, 1–34. (b) Sogah, D. Y.; Hertler, W. R.; Webster, O. W.; Cohen, G. M. *Macromolecules* **1987**, *20*, 1473–1488. (c) Webster, O. W.; Hertler, W. R.; Sogah, D. Y.; Farnham, W. B.; RajanBabu, T. V. *J. Am. Chem. Soc.* **1983**, *105*, 5706–5708.

(13) Kakuchi, R.; Chiba, K.; Fuchise, K.; Sakai, R.; Satoh, T.; Kakuchi, T. *Macromolecules* **2009**, *42*, 8747–8750.

(14) Mathieu, B.; Ghosez, L. *Tetrahedron Lett.* **1997**, *38*, 5497–5500.

(15) Fuchise, K.; Sakai, R.; Satoh, T.; Sato, S.-I.; Narumi, A.; Kawaguchi, S.; Kakuchi, T. *Macromolecules* **2010**, *43*, 5589–5594.

(16) (a) Yamamoto, H. *Tetrahedron* **2007**, *63*, 8377–8412. (b) Boxer, M. B.; Yamamoto, H. *J. Am. Chem. Soc.* **2006**, *128*, 48–49. (c) Ishihara, K.; Hiraiwa, Y.; Yamamoto, H. *Synlett* **2001**, 1851–1854.

(17) Zhang, Y.; Lay, F.; García-García, P.; List, B.; Chen, E. Y.-X. *Chem.—Eur. J.* **2010**, *16*, 10462–10473.

(18) Chen, E. Y.-X.; Marks, T. J. *Chem. Rev.* **2000**, *100*, 1391–1434.

(19) Jutzi, P.; Müller, C.; Stammler, A.; Stammler, H. *Organometallics* **2000**, *19*, 1442–1444.

(20) (a) Tjaden, E. B.; Swenson, D. C.; Jordan, R. F. *Organometallics* **1995**, *14*, 371–386.(b) Turner, H. W.; Hlatky, G. G.; Eckman, R. R. U.S. Patent 5,198,401, 1993.

(21) Ute, K.; Ohnuma, H.; Kitayama, T. *Polym. J.* **2000**, *32*, 1060–1062.

(22) Zhuang, R.; Müller, A. H. E. *Macromolecules* **1995**, *28*, 8035—8042; 8043—8050.

(23) Ute, K.; Ohnuma, H.; Shimizu, I.; Kitayama, T. *Polym. J.* **2006**, *38*, 999–1003.

(24) Miyake, G. M.; Zhang, Y.; Chen, E. Y.-X. *Macromolecules* **2010**, *43*, 4902–4908.

(25) (a) Coates, G. W.; Hillmyer, M. A. *Macromolecules* **2009**, *42*, 7987–7989. (b) Gandini, A. *Macromolecules* **2008**, *41*, 9491–9504. (c) Tullo, A. H. *C&E News* **2008**, *86* (39), 21–25. (d) Williams, C. K.; Hillmyer, M. A. *Polym. Rev.* **2008**, *48*, 1–10. (e) Meier, M. A. R.; Metzger, J. O.; Schubert, S. *Chem. Soc. Rev.* **2007**, *36*, 1788–1802.

(26) Mullin, R. *C&E News* **2004**, *82* (45), 29–37.

(27) Hoffman, H. M. R.; Rabe, J. *Angew. Chem., Int. Ed. Engl.* **1985**, *24*, 94–110.

(28) (a) Manzer, L. E. *ACS Symp. Ser.* **2006**, *921*, 40–51. (b) Manzer, L. E. *Appl. Catal. A: Gen.* **2004**, *272*, 249–256.

(29) For selected examples, see: (a) Cockburn, R. A.; Siegmann, R.; Payne, K. A.; Beuermann, S.; McKenna, T. F. L.; Hutchinson, R. A. *Biomacromolecules* **2011**, *12*, 2319–2326. (b) Juhari, A.; Mosnáček, J.; Yoon, J. A.; Nese, A.; Koynov, K.; Kowalewski, T.; Matyjaszewski, K. *Polymer* **2010**, *51*, 4806–4813. (c) Cockburn, R. A.; McKenna, T. F. L.; Hutchinson, R. A. *Macromol. Chem. Phys.* **2010**, *211*, 501–509. (d) Mosnáček, J.; Yoon, J. A.; Juhari, A.; Koynov, K.; Matyjaszewski, K. *Polymer* **2009**, *50*, 2087–2094. (e) Mosnáček, J.; Matyjaszewski, K. *Macromolecules* **2008**, *41*, 5509–5511. (f) Qi, G.; Nolan, M.; Schork, F. J.; Jones, C. W. *J. Polym. Sci.: Polym. Chem.* **2008**, *46*, 5929–5944. (g) Bandenburg, C. J. U.S. Patent 6,841,627 B2, 2005. (h) Gridnev, A. A.; Ittel, S. D. WO 035960 A2, 2000. (i) Stansbury, J. W.; Antonucci, J. M. *Dent. Mater.* **1992**, *8*, 270–273. (j) Ueda, M.; Takahashi, M.; Imai, Y.; Pittman, C. U., Jr. *J. Polym. Sci.: Polym. Chem. Ed.* **1982**, *20*, 2819–2828. (k) Akkapeddi, M. K. *Polymer* **1979**, *20*, 1215–1216. (l) Akkapeddi, M. K. *Macromolecules* **1979**, *12*, 546–551.

(30) Suenaga, J.; Sutherlin, D. M.; Stille, J. K. *Macromolecules* **1984**, *17*, 2913–2916.

(31) Hu, Y.; Gustafson, L. O.; Zhu, H.; Chen, E. Y.-X. *J. Polym. Sci., Part A: Polym. Chem.* **2011**, *49*, 2008–2017.

(32) Zhang, Y.; Miyake, G. M.; Chen, E. Y.-X. *Angew. Chem., Int. Ed.* **2010**, *49*, 10158–10162.

(33) Miyake, G. M.; Newton, S. E.; Mariott, W. R.; Chen, E. Y.-X. *Dalton Trans.* **2010**, *39*, 6710–6718.

(34) Hu, Y.; Xu, X.; Zhang, Y.; Chen, Y.; Chen, E. Y.-X. *Macromolecules* **2010**, *43*, 9328–9336.

(35) Delferro, M.; Marks, T. J. *Chem. Rev.* **2011**, *111*, 2450–2485.

(36) Allen, R. D.; Long, T. E.; McGrath, J. E. *Polym. Bull.* **1986**, *15*, 127–134.

(37) (a) Bochmann, M.; Lancaster, S. J. *J. Organomet. Chem.* **1992**, *434*, C1–C5. (b) Chien, J. C. W.; Tsai, W.-M.; Rausch, M. D. *J. Am. Chem. Soc.* **1991**, *113*, 8570–8571.

(38) (a) Favarger, F.; Ginglinger, C. G.; Monchaud, D.; Lacour, J. *J. Org. Chem.* **2004**, *69*, 8521–8524. (b) Lee, H. S.; Novak, B. *Polym. Prepr.* **2005**, *46*, 839–840.

(39) (a) Rodriguez-Delgado, A.; Chen, E. Y.-X. *J. Am. Chem. Soc.* **2005**, *127*, 961–974. (b) Rodriguez-Delgado, A.; Chen, E. Y.-X. *Macromolecules* **2005**, *38*, 2587–2594.

(40) (a) Rodriguez-Delgado, A.; Mariott, W. R.; Chen, E. Y.-X. *Macromolecules* **2004**, *37*, 3092–3100. (b) Bolig, A. D.; Chen, E. Y.-X. *J. Am. Chem. Soc.* **2004**, *126*, 4897–4906. (c) Brar, A. S.; Singh, G.; Shankar, R. *J. Mol. Struct.* **2004**, *703*, 69–81.(d) Bovey, F. A.; Mirau, P. A. *NMR of Polymers*; Academic Press: San Diego, CA, 1996. (e) Kawamura, T.; Toshima, N.; Matsuzaki, K. *Makromol. Chem., Rapid Commun.* **1993**, *14*, 719–724. (f) Chujo, R.; Hatada, K.; Kitamaru, R.; Kitayama, T.; Sato, H.; Tanaka, Y. *Polym. J.* **1987**, *19*, 413–424. (g) Ferguson, R. C.; Ovenall, D. W. *Macromolecules* **1987**, *20*, 1245–1248.

(41) Fukuzumi, S.; Ohkubo, K.; Otera, J. *J. Org. Chem.* **2001**, *66*, 1450–1454.

(42) Stojcevic, G.; Kim, H.; Taylor, N. J.; Marder, T. B.; Collins, S. *Angew. Chem., Int. Ed.* **2004**, *43*, 5523–5526.

(43) Zhang, Y.; Ning, Y.; Caporaso, L.; Cavallo, L.; Chen, E. Y.-X. *J. Am. Chem. Soc.* **2010**, *132*, 2695–2709.